



## OPEN Clinical characteristics of disc hemorrhages depending on their locations and glaucoma progression in myopic patients

Seong Ah Kim<sup>1</sup>, Hee Jong Shin<sup>1</sup>, Hee Kyoung Ryu<sup>1</sup>, Chan Kee Park<sup>1</sup> & Hae-Young Lopilly Park<sup>1,2</sup>✉

This study aimed to investigate clinical characteristics and glaucoma progression in eyes with disc hemorrhage (DH) in the region of peripapillary atrophy (PPA) or DH in temporal region among glaucoma patients with myopia. One hundred ninety-six eyes of 196 glaucoma patients with myopia who were observed at least 4 years and had more than six visual field (VF) tests were included. Eyes with DHs located in the optic disc region at the superotemporal or inferotemporal locations were defined as typical DH. PPA area, disc ovality ratio, and disc torsion were measured. Length of  $\gamma$ -zone PPA, distance from disc edge to fovea, angle of scleral bending were measured using optical coherence tomography. Comparison of baseline characteristics between eyes with and without DH in PPA/DH in temporal region showed similar axial length ( $26.95 \pm 1.60$  mm;  $26.82 \pm 1.07$  mm).  $\gamma$ -zone PPA was longer and angle of scleral bending was larger in eyes with DH in PPA/DH in temporal region (both  $p \leq 0.001$ ). Longer  $\gamma$ -zone PPA ( $\beta = 1.001$ ;  $p = 0.018$ ) and larger angle of scleral bending ( $\beta = 1.033$ ;  $p = 0.008$ ) were associated with presence of DH in PPA/DH in temporal region using logistic regression analysis. Eyes with DH in PPA/DH in temporal region had a smaller mean deviation slope of VF, a larger disc ovality ratio, a longer  $\gamma$ -zone PPA, and a larger PPA area when compared to those of eyes typical DH. VF progression was associated with absence of DH in PPA/DH in temporal region ( $p = 0.030$ ) and larger angle of scleral bending ( $p = 0.019$ ) using Cox proportional hazards model. DH in PPA/DH in temporal region was associated with stretching and deformation of sclera that may be result from myopic changes. Associated factors with VF progression was the degree of scleral deformation, not the presence of DH in PPA/DH in temporal region, showing that DH related to scleral deformation may possess clinical significance in glaucoma with myopia.

Disc hemorrhage (DH) is significant risk factor for development and progression of glaucoma, typically located on or at the margin of optic disc<sup>1–3</sup>. In the Early Manifest Glaucoma Trial and Collaborative Normal-Tension Glaucoma Study (CNTGS), it was significantly associated with glaucoma progression<sup>4,5</sup>. Several studies reported that occurrence of DH was associated with new RNFL defect, the enlargement of RNFL defect, lamina disinsertion, and visual field (VF) progression<sup>6–8</sup>.

The majority of earlier studies on DHs were usually performed in glaucoma cohorts, and eyes with high myopia were usually excluded from the DH studies, although myopia was only considered as an influencing factor for development of glaucoma<sup>9–11</sup>. A previous report showed that DH in myopic eyes had higher proportion to be found at the cup area within the lamina cribrosa<sup>12</sup>. Reports about the clinical significance of DH in myopic eyes were controversial and one study showed DH in mild-to-moderate myopia was associated with structural progression, however, not with functional progression<sup>13</sup>.

Classically, DHs associated with glaucoma are mostly found in the superotemporal or inferotemporal regions of optic disc, especially in the 7 o'clock sector<sup>14,15</sup>. We observed that the DHs are often located in the peripapillary atrophic (PPA) areas or temporal regions of optic disc, as well as in superotemporal or inferotemporal regions. In addition, Xiong et al<sup>16</sup> reported that DHs were most often located in the peripapillary atrophic (PPA) areas especially in their temporal regions in eyes with pathologic myopia. There is a previous study showing that DH

<sup>1</sup>Department of Ophthalmology, Seoul St. Mary's Hospital, College of Medicine, The Catholic University of Korea, Seoul, Republic of Korea. <sup>2</sup>Department of Ophthalmology and Visual Science, Seoul St. Mary's Hospital, College of Medicine, The Catholic University of Korea, 505 Banpo-dong, Seocho-gu, Seoul 137-701, Korea. ✉email: lopilly@catholic.ac.kr

at the superotemporal or inferotemporal location were associated with glaucoma progression compared to DH in the temporal area and the latter eyes had greater tilt ratio<sup>17</sup>.

The present study aimed to investigate associated factors with DH in PPA and determine whether it was associated with progression of glaucoma in terms of changes of VF parameters in eyes with myopia.

## Results

A total of 210 eyes of 210 open-angle glaucoma patients with myopia who met the inclusion and exclusion criteria were included. Of the 210 eyes, 14 eyes were excluded from final analyses because the optical coherence tomography (OCT) images were of poor quality or had motion artifacts. 47 eyes with DH in PPA/DH in temporal region, 50 eyes with typical DH, and 99 eyes without DH were included. Among 47 eyes with DH in PPA, 12 eyes presented with DH in PPA and 35 eyes presented with DH at the temporal side of optic nerve head (ONH) along peripapillary or rim of optic disc. Interobserver agreement were 0.937 (95% confidence interval [CI], 0.896–0.977) for PPA area measurements from disc photography images, 0.917 (95% CI, 0.887–0.946) for length of  $\gamma$ -zone PPA measurements from OCT images, and 0.907 (95% CI, 0.890–0.934) for angle of scleral bending measurements from OCT images.

Baseline patient characteristics are listed in Table 1. There was no difference between eyes with DH in PPA and without DH in terms of mean age at diagnosis ( $50.31 \pm 12.03$  years, eyes without DH;  $54.23 \pm 10.92$  years, eyes with DH;  $p=0.060$ ), axial length ( $26.82 \pm 1.07$  mm, eyes without DH;  $26.95 \pm 1.60$  mm, eyes with DH,  $p=0.574$ ), baseline RNFL thickness ( $71.43 \pm 19.98\mu\text{m}$ , eyes without DH,  $76.72 \pm 12.13\mu\text{m}$ , eyes with DH,  $p=0.097$ ), MD (mean deviation) of VF ( $-6.91 \pm 4.81\text{dB}$ , eyes without DH,  $-8.04 \pm 6.55\text{dB}$ , eyes with DH,  $p=0.298$ ), disc ovality ratio ( $1.42 \pm 0.26$ , eyes without DH,  $1.48 \pm 0.31$ , eyes with DH,  $p=0.200$ ), disc torsion ( $12.76 \pm 10.09^\circ$ , eyes without DH,  $9.60 \pm 15.70^\circ$ , eyes with DH,  $p=0.724$ ), PPA area ( $34222.61 \pm 19717.85$  pixel, eyes without DH,  $68831.43 \pm 93851.61$  pixel, eyes with DH,  $p=0.724$ ) and distance from disc edge to fovea ( $4478.53 \pm 458.98\mu\text{m}$ , eyes without DH,  $4649.82 \pm 629.09\mu\text{m}$ , eyes with DH,  $p=0.100$ ). However, eyes with DH in PPA/DH in temporal region showed lower baseline IOP, longer  $\gamma$ -zone, and larger angle of scleral bending compared with those in eyes without DH ( $p=0.042$ ,  $p=0.032$ , and  $p=0.001$ ).

To identify factors associated with DH in PPA/DH in temporal region in myopic eyes, we performed logistic regression analyses (Table 2). Longer  $\gamma$ -zone PPA ( $\beta$ , 1.001; 95% CI, 1.000–1.003;  $p=0.018$ ) and larger angle of scleral bending ( $\beta$ , 1.033; 95% CI, 1.008–1.059;  $p=0.008$ ) were significantly associated with presence of DH in PPA/DH in temporal region in univariate and multivariate analyses.

Among 47 eyes with DH in PPA/DH in temporal region, 10 eyes were excluded as loss to follow-up. There was no difference in terms of mean IOP during follow-up between DH in PPA/DH in temporal region group ( $13.77 \pm 2.82\text{mmHg}$ ) and no DH group ( $14.78 \pm 3.81\text{mmHg}$ ;  $p=0.068$ ). To identify factors associated with progression of glaucoma as measured with VF, we performed Cox proportional hazard analysis shown in Table 3. Longer axial length, worse baseline MD in VF, and smaller disc torsion, meaning greater disc torsion to the inferotemporal direction, were associated with VF progression in univariate cox proportional analyses ( $p=0.008$ ;  $p=0.014$ ; and  $p=0.013$ ). However, no significant correlation was observed for any included factor in multivariate analyses.

A comparison of baseline characteristics was performed based on location of DH to identify its relations with glaucoma progression (Table 4). Patients with DH in PPA/DH in temporal region were older and observed

	Eyes without disc hemorrhage ( <i>n</i> = 99)	Eyes with disc hemorrhage in PPA/Disc hemorrhage in temporal region ( <i>n</i> = 47)	<i>P</i> value
Age, y	50.31 ± 12.03	54.23 ± 10.92	0.060 <sup>a</sup>
Female, No. (%)	56 (56.5)	30 (63.8)	0.405 <sup>b</sup>
Axial length, mm	26.82 ± 1.07	26.95 ± 1.60	0.574 <sup>a</sup>
Central corneal thickness, $\mu\text{m}$	517.45 ± 50.41	507.17 ± 45.62	0.241 <sup>a</sup>
Best corrected visual acuity, Snellen	0.77 ± 0.11	0.82 ± 0.23	0.152 <sup>a</sup>
Spherical equivalent, Diopters	-5.18 ± 3.50	-5.10 ± 4.25	0.898 <sup>a</sup>
<b>Baseline intraocular pressure, mmHg</b>	14.88 ± 3.85	13.72 ± 2.79	<b>0.042<sup>a</sup></b>
Baseline RNFL thickness, $\mu\text{m}$	71.43 ± 19.98	76.72 ± 12.13	0.097 <sup>a</sup>
Baseline mean deviation of VF, dB	-6.91 ± 4.81	-8.04 ± 6.55	0.298 <sup>a</sup>
Baseline pattern standard deviation of VF, dB	7.98 ± 5.81	7.61 ± 4.78	0.681 <sup>a</sup>
Disc ovality ratio	1.42 ± 0.26	1.48 ± 0.31	0.200 <sup>a</sup>
Disc torsion, degrees	12.76 ± 10.09	9.60 ± 15.70	0.211 <sup>a</sup>
PPA area, pixel	34222.61 ± 19717.85	68831.43 ± 93851.61	0.724 <sup>a</sup>
<b><math>\gamma</math>-zone PPA, <math>\mu\text{m}</math></b>	378.25 ± 276.36	680.03 ± 526.99	<b>&lt; 0.001<sup>a</sup></b>
Distance from the disc edge to the foveal center, $\mu\text{m}$	4478.53 ± 458.98	4649.82 ± 629.09	0.100 <sup>a</sup>
<b>Angle of scleral bending, degrees</b>	32.97 ± 16.69	50.82 ± 31.39	<b>0.001</b>

**Table 1.** Comparison of the demographics and baseline characteristics between eyes with and without disc hemorrhage in PPA. RNFL, retinal nerve fiber layer; VF, visual field; PPA, peripapillary atrophy. Data are presented as mean ± standard deviation (range) unless otherwise indicated. <sup>a</sup> Student *t* test. <sup>b</sup> Chi-square test. Factors with statistical significance are shown in bold.

	Univariate $\beta$ (95% CI)	P value	Multivariate $\beta$ (95% CI)	P value
Age, y	1.020 (0.977–1.065)	0.368		
Female, No.	1.053 (0.421–2.633)	0.282		
Diabetes mellitus, n	1.498 (0.196–11.437)	0.697		
Hypertension, n	0.487 (0.038–6.248)	0.581		
Baseline intraocular pressure, mmHg	0.926 (0.806–1.065)	0.282		
Axial length, mm	0.612 (0.354–1.058)	0.179		
Baseline RNFL thickness, $\mu\text{m}$	1.023 (0.976–1.074)	0.344		
Baseline mean deviation of VF, dB	0.933 (0.846–1.029)	0.167		
Disc ovality ratio	0.156 (0.009–2.805)	0.208		
Disc torsion, degrees	0.988 (0.947–1.032)	0.590		
<b><math>\gamma</math>-zone PPA, <math>\mu\text{m}</math></b>	1.003 (1.001–1.005)	<b>&lt; 0.001</b>	1.001 (1.000–1.003)	<b>0.018</b>
PPA area, pixel	1.002 (0.999–1.005)	0.304		
Distance from the disc edge to the foveal center, $\mu\text{m}$	1.000 (0.998–1.001)	0.538		
<b>Angle of scleral bending, degrees</b>	1.038 (1.013–1.064)	<b>0.003</b>	1.033 (1.008–1.059)	<b>0.008</b>

**Table 2.** Factors associated with presence of disc hemorrhage in peripapillary atrophy or in temporal region using logistic regression analysis. RNFL, retinal nerve fiber layer; VF, visual field; PPA, peripapillary atrophy. Factors with  $P < 0.1$  in univariate analysis were included in multivariate analysis. Factors with statistical significance are shown in bold.

	Univariate HR (95% CI)	P value	Multivariate HR (95% CI)	P value
Presence of Disc hemorrhage in PPA/Disc hemorrhage in temporal region	0.432 (0.145–1.285)	<b>0.069</b>	0.905 (0.247–3.311)	0.880
Age, y	1.012 (0.960–1.068)	0.651		
Diabetes mellitus, n	2.116 (0.261–17.121)	0.482		
Hypertension, n	1.556 (0.201–12.039)	0.672		
Axial length, mm	1.612 (1.130–2.299)	<b>0.008</b>	1.350 (0.889–2.029)	0.148
Baseline mean deviation of VF, dB	0.896 (0.822–0.978)	<b>0.014</b>	0.942 (0.858–1.033)	0.202
Mean IOP during follow-up, mmHg	1.079 (0.928–1.256)	0.323		
Disc ovality ratio	4.289 (0.390–47.128)	0.234		
Disc torsion, degrees	0.935 (0.5887–0.986)	<b>0.013</b>	0.948 (0.893–1.007)	0.082
$\gamma$ -zone PPA, $\mu\text{m}$	1.000 (0.998–1.001)	0.728		
PPA area, pixel	1.000 (1.000–1.000)	0.411		
Distance from the disc edge to the foveal center, $\mu\text{m}$	1.000 (0.999–1.001)	0.816		
Angle of scleral bending, degrees	1.011 (0.991–1.031)	0.295		

**Table 3.** Factors associated with progression of glaucoma as measured with VF using Cox Proportional Hazard analysis. PPA, peripapillary atrophy; VF, visual field; IOP, intraocular pressure. Factors with  $P < 0.1$  in univariate analysis were included in multivariate analysis.

with smaller MD slope, larger disc ovality ratio, longer  $\gamma$ -zone PPA, and larger PPA area ( $p = 0.021$ ;  $p = 0.002$ ;  $p = 0.001$ ;  $p < 0.001$ ;  $p < 0.001$ , respectively) than eyes with typical DH. Cox proportional hazard analyses were performed to identify the factors associated with VF progression in eyes with DH distinguished by its location (Table 5). Absence of DH in PPA/DH in temporal region was significantly associated with VF progression in that presence of typical DH was associated with VF progression in multivariate analysis (HR 0.296; 95% CI 0.099–0.890,  $p = 0.030$ ). Larger angle of scleral bending was associated with VF progression (HR 1.026; 95% CI 1.004–1.048;  $p = 0.019$ ).

Representative cases are shown in Fig. 1. In the upper case, a 65-year-old woman had normal tension glaucoma with myopia in her left eye with DH in PPA. In the bottom case, a 68-year-old woman with normal tension glaucoma with myopia in her left eye with DH located at inferotemporal region on neuroretinal rim. The eye in the upper case had similar axial length, longer  $\gamma$ -zone PPA, and larger angle of scleral bending compared with those in the bottom case. The VF did not show progression in the upper case, whereas VF progression occurred in the bottom case during follow-up period.

## Discussion

In this study, we found that the presence of DH in PPA/DH in temporal region was associated with longer  $\gamma$ -zone PPA and larger angle of scleral bending, although it was not associated with VF progression in eyes with and without DH in PPA/DH in temporal region. When comparing eyes with DH in PPA/DH in temporal region

	Typical disc hemorrhage (n = 50)	Disc Hm in PPA/Disc hemorrhage in temporal region (n = 37)	P value
Age, y	59.58 ± 10.95	54.16 ± 10.06	<b>0.021<sup>a</sup></b>
Female, No. (%)	36 (72.0)	25 (67.5)	0.575 <sup>b</sup>
Diabetes mellitus, No. (%)	1 (2.0)	2 (5.4)	0.389 <sup>b</sup>
<b>Hypertension, No. (%)</b>	13 (26.0)	1 (2.7)	<b>0.030<sup>b</sup></b>
Axial length, mm	26.66 ± 1.72	26.93 ± 1.61	0.461 <sup>a</sup>
Mean IOP during follow-up, mmHg	13.22 ± 2.57	13.73 ± 2.58	0.365 <sup>a</sup>
Follow-up duration, y	7.258 ± 2.59	6.68 ± 2.84	0.317 <sup>a</sup>
Baseline RNFL thickness, µm	73.60 ± 10.65	70.11 ± 11.26	0.144 <sup>a</sup>
Baseline MD of VF, dB	-6.67 ± 4.61	-7.23 ± 5.72	0.627 <sup>a</sup>
<b>MD slope of VF</b>	<b>-0.57 ± 0.52</b>	<b>-0.06 ± 0.95</b>	<b>0.002<sup>a</sup></b>
No of VF examination	6.38 ± 2.04	5.71 ± 2.63	0.214 <sup>b</sup>
<b>Disc ovality ratio</b>	<b>1.29 ± 0.22</b>	<b>1.50 ± 0.29</b>	<b>0.001<sup>a</sup></b>
Disc torsion, degrees	19.59 ± 7.93	16.39 ± 9.32	0.089 <sup>a</sup>
<b>γ-zone PPA, µm</b>	<b>324.64 ± 344.04</b>	<b>673.49 ± 463.38</b>	<b>&lt; 0.001<sup>a</sup></b>
<b>PPA area, pixel</b>	<b>2620.41 ± 2072.98</b>	<b>61066.85 ± 76888.60</b>	<b>&lt; 0.001<sup>a</sup></b>
Distance from the disc edge to the foveal center, µm	4370.56 ± 1110.31	4632.67 ± 559.17	0.192 <sup>a</sup>
Angle of scleral bending, degrees	38.56 ± 14.06	47.06 ± 30.41	0.121 <sup>a</sup>

**Table 4.** Comparison of clinical characteristics between disc hemorrhage in peripapillary atrophy and typical disc hemorrhage. IOP, intraocular pressure; RNFL, retinal nerve fiber layer; MD, mean deviation; VF, visual field; PPA, peripapillary atrophy. Data are presented as mean ± standard deviation (range) unless otherwise indicated. <sup>a</sup> Student *t* test. <sup>b</sup> Chi-square test. Factors with statistical significance are shown in bold.

	Univariate HR (95% CI)	P value	Multivariate HR (95% CI)	P value
<b>Presence of disc hemorrhage in PPA/Disc hemorrhage in temporal region</b>	0.311 (0.120–0.806)	<b>0.016</b>	0.296 (0.099–0.890)	<b>0.030</b>
Age, y	1.030 (0.999–1.061)	<b>0.058</b>	1.017 (0.983–1.051)	0.332
Diabetes mellitus, No.	0.048 (0.000–42.572)	0.710		
Hypertension, No.	1.729 (0.692–4.319)	0.241		
Axial length, mm	1.007 (0.831–1.220)	0.942		
Baseline MD of VF, dB	0.945 (0.884–1.011)	0.103		
Mean IOP during follow-up, mmHg	1.035 (0.914–1.171)	0.588		
Disc ovality ratio	0.507 (0.103–2.488)	0.403		
Disc torsion, degrees	0.995 (0.952–1.040)	0.823		
γ-zone PPA, µm	0.999 (0.998–1.000)	<b>0.065</b>	1.000 (0.999–1.002)	0.632
PPA area, pixel	1.000 (1.000–1.000)	0.211		
Distance from the disc edge to the foveal center, µm	0.999 (0.999–1.000)	<b>0.076</b>	0.999 (0.999–1.000)	0.093
<b>Angle of scleral bending, degrees</b>	1.016 (0.994–1.038)	<b>0.049</b>	1.026 (1.004–1.048)	<b>0.019</b>

**Table 5.** Factors associated with progression of glaucoma as measured with VF using Cox Proportional Hazard analysis. PPA, peripapillary atrophy; MD, mean deviation; VF, visual field; IOP, intraocular pressure. Factors with  $P < 0.1$  in univariate analysis were included in multivariate analysis. Factors with statistical significance are shown in bold.

and typical DH to identify clinical significance depending on the location of DH in myopia, patients with DH in PPA/DH in temporal region was younger, had less hypertension, and showed smaller MD slope of VF, larger disc ovality ratio, longer γ-zone PPA, and larger PPA area. VF progression was associated with larger scleral bending and absence of DH in PPA/DH in temporal region, which in turn means that the presence of typical DH was associated with VF progression.

In DH in PPA group, 12 eyes presented with DH in PPA and 35 eyes presented with DH at the temporal side of ONH extending to the PPA region. In myopic eyes, axial elongation leads to an enlargement of the globes mainly in its posterior region, and at the temporal region of the ONH<sup>18</sup>. Previous studies also reported that the γ-zone PPA developed and enlarged temporally from the disc border in myopic eyes and progresses predominantly temporal to ONH<sup>19–21</sup>. Xiong et al<sup>16</sup>. also reported that DHs in myopic eyes were most frequently observed at temporal to ONH. We hypothesized that a DH located not only in PPA but also at temporal to optic disc may be relevant to scleral stretching or distortion related to myopia.

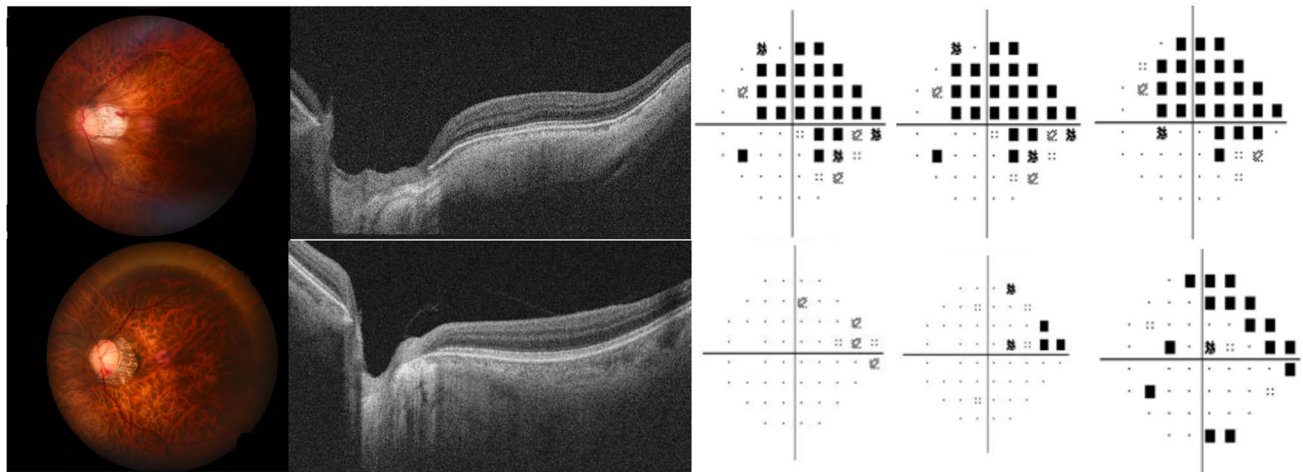


**Figure 1.** A 65-year-old woman with normal tension glaucoma in her left eye with disc hemorrhage in peripapillary atrophy (PPA) (the upper case). Axial length was 28.09 mm, the length of  $\gamma$ -zone PPA was 1264  $\mu\text{m}$ , and angle of scleral bending was 45.00 degrees. The visual field did not show progression during 3-year follow-up period. A 68-year-old woman with normal tension glaucoma in her left eye with disc hemorrhage located at inferotemporal region on neuroretinal rim (the lower case). Axial length was 27.97 mm, the length of PPA was 599  $\mu\text{m}$ , and angle of scleral bending was 18.24 degrees. The visual field showed progression in the superior arcuate area during 3-year follow-up period.

The earlier suggested pathogenesis of DHs in glaucoma patients<sup>22</sup> may not be appropriate for DHs in myopic eyes or in the PPA area. Quigley et al<sup>23</sup> suggested that DH is a mechanical rupture of the small blood vessels at the level of the lamina cribrosa (LC) in that enlargement of RNFL defect causes damage or loss of capillaries at the border of a RNFL defect. This may be explained that structural alteration resulting in mechanical rupture of the vessels leading to DH. DHs were more commonly found within LC in myopic eyes than in non-myopic eyes<sup>12</sup>. Xiong and colleagues<sup>16</sup> classified DHs in eyes with pathologic myopia and found that DHs were most often located in the PPA region and the temporal side, respectively. DHs are mostly located in temporal side and developed in the areas of straightened retinal arterioles, at or beside the peak of a ridge, in an area of compressed retinal tissue. They suggested that it may be mainly related to the mechanical tension generated by PM-associated lesions. In this study, the presence of a DH in PPA is associated with longer  $\gamma$ -zone PPA and larger angle of scleral bending regardless of axial length. A  $\gamma$ -zone PPA is associated with axial elongation resulting from a stretching of the temporal peripapillary scleral flange<sup>24,25</sup>. In addition, the degree of scleral deformation near ONH represented by angle of scleral bending was associated DH in PPA. Akagi and associates evaluated scleral bending and its angle temporal to the ONH to evaluate scleral deformation identified on SS OCT observation<sup>26</sup>. Stretching and deformation of sclera were associated with presence of DH in PPA, and it may be related to the mechanical forces, tensile strength or compression, generated by myopia-associated lesions, leading to directly or indirectly damage the vessels.

It is known that DHs are associated with progression of glaucoma<sup>5,27</sup>. It was demonstrated that glaucoma eyes with DH at the site of focal LC defects showed frequent and faster VF progression compared with DH not accompanied by LC alterations or LC alterations not accompanied by DH<sup>10</sup>. RNFL defects are frequently found in the inferotemporal region, followed by the superotemporal region, but rarely observed in the temporal region of PPA area<sup>28</sup>. Hsia et al<sup>17</sup> reported that DHs in the superotemporal and inferotemporal regions had more structural and functional glaucoma deterioration compared with the eyes with DHs in the temporal and nasal area, and the latter eyes had greater disc tilt ratio. In this study, eyes with typical DHs located at the superotemporal or inferotemporal to ONH showed VF progression, but eyes with DHs in PPA/DH in temporal region did not. DHs in PPA or temporal region are not located at glaucomatous damage sites. Instead, they are associated with scleral stretching and deformation resulting from myopic axial elongation. Therefore, VF progression may not occur from stretching of the tissues, but associated with deformation of sclera by eyeball elongation. A study by Yamagami was consistent with our findings in that the association of DH occurrence and glaucoma progression was evident in non-myopic glaucomatous disc, but not in myopic glaucomatous disc<sup>29</sup>.

Ohno-Matsui and associates demonstrated that an abrupt change in the scleral curvature temporal to the optic disc in eyes with high myopia was associated with progressive visual field defects on Goldmann perimetry<sup>30</sup>. As accordance with the previous study, VF progression was associated with larger angle of scleral bending. In our study, typical DHs located in the inferotemporal or superotemporal region, which are known to be vulnerable to mechanical damage including compression and deformation of the LC, were associated with VF progression, whereas DH in PPA/DH in temporal region was not. The presence of DH in PPA/DH in temporal region was associated with longer  $\gamma$ -zone PPA and larger angle of scleral bending. Altogether, it could be postulated that elongation and deformation of the temporal peripapillary sclera could result DH in these regions, however, DH in PPA/DH in temporal region is not cause or result of glaucomatous progression. Pathogenesis underlying



glaucomatous damage and progression in myopic eyes may not simply associated with stretching of sclera, but deformation of the peripapillary sclera associated with the vulnerability of the ONH.

Our study has several limitations. First, there was a small number of eyes with DHs in PPA. The majority of DHs was located in temporal regions in the DH in PPA group/DH in temporal region. We supposed that DHs in PPA as well as DHs in temporal regions may be related with myopic degeneration. In this study, we aimed to identify the clinical characteristics of DHs frequently observed in myopic eyes, specifically those not located in the superotemporal or inferotemporal regions. Further studies on the DHs solely in PPA are needed in the future. Second, DHs might have been missed during the interval. DHs usually last for approximately 6 to 12 months<sup>31</sup>, and the follow-up interval was 6 to 12 months in our study. Third, the frequency of follow-ups could affect the detection of DH and glaucoma progression. We included patients with minimum of six VFs, and these VF examinations were usually performed at 6- to 12-month intervals. More frequent VF testing to detect VF progression using linear regression analysis is suggested. We analyzed global MD rates of change to compare the rate of progression between groups. Lastly, we made an effort to include only typical glaucomatous VF defects such as paracentral defect, nasal step, partial arcuate defect, and, arcuate defect. We carefully examined to exclude myopia-related defects (temporal field loss, enlarged blind spot) described in the earlier study<sup>32</sup>. In addition, pathologic myopia with other retinal lesions was excluded with the assistance of retinal specialists.

In conclusion, DH in PPA and those located at temporal region were associated with longer  $\gamma$ -zone PPA and larger angle of scleral bending, indicative of stretching and deformation of sclera. Eyes with DH in PPA/DH in temporal region showed less VF progression when compared with eyes with typical DH. The pathogenesis of DHs in PPA is probably different from typical DHs. It may be mainly related to mechanical stress generated by scleral deformation associated with myopia, not directly with axial length. In addition, it was not associated with glaucoma progression, distinguishing it from typical DH. This may suggest that the degree of scleral deformation has clinical significance in terms of progression, not simply the presence of DH in PPA by scleral stretching, showing that DH related to scleral deformation may possess clinical significance in glaucoma with myopia.

## Methods

### Subjects

We retrospectively reviewed the medical records of 210 glaucoma patients with myopia who were observed with or without DH during the follow-up, from January 2014 to December 2021 at Seoul St. Mary's Hospital. Patients who were followed up for at least 4 years with visits at 2- to 6-month intervals after the initial visit were selected for the study. This study followed the tenets of the Declaration of Helsinki. The study was approved by the Institutional Review Board of Seoul St. Mary's Hospital (KC23RASI0309) by following all guidelines for experimental investigation in human subjects. We enrolled all consecutive eligible patients who were willing to participate, and all gave written informed consent.

For the initial evaluation, each patient received a complete ophthalmic examination, including a review of the medical history, measurement of best-corrected visual acuity, refraction, slit-lamp biomicroscopy, gonioscopy, Goldmann applanation tonometry, central corneal thickness using ultrasound pachymetry (Tomey Corporation, Nagoya, Japan), dilated stereoscopic examination of the optic disc, disc and red-free fundus photography (Canon, Tokyo, Japan), Cirrus OCT (Carl Zeiss Meditec), Humphrey VF examination using the Swedish Interactive Thresholding Algorithm Standard 24-2 test (Carl Zeiss Meditec). Measurement of axial length was performed using ocular biometry (IOLMaster; Carl Zeiss Meditec), and only patients with axial length of  $\geq 25$  mm were included. During the follow-up period, patients were examined using serial disc and red-free fundus photography, IOP measurements with intervals of  $6 \pm 2$  months, and VF examinations regularly with intervals of  $12 \pm 2$  months.

Patients underwent examinations to fulfill following criteria: an open angle on gonioscopic examination, glaucomatous optic disc appearance (such as diffuse or localized rim thinning, a notch in the rim, or a vertical cup to disc ratio higher than 0.6, or higher than that of the other eye by more than 0.2), and glaucomatous VF loss (a cluster of 3 points with a probability of  $< 5\%$  on the pattern deviation map in  $> 1$  hemifield, including  $> 1$  point with a probability of  $< 1\%$ ; or a cluster of 2 points with a probability of  $< 1\%$  on 2 qualifying VFs), both confirmed by 2 glaucoma specialists (S.A.K and H-Y.L.P).

Patients were excluded if they had any of the following criteria: (1) a history of any retinal disease, including diabetic or hypertensive retinopathy, (2) a history of eye trauma or surgery, with the exception of uncomplicated cataract surgery, (3) other optic nerve diseases besides glaucoma, (4) and a history of systemic or neurological diseases that might affect the VF.

### Diagnosis of disc hemorrhage

DH was evaluated based on optic disc photographs during follow-up and confirmed by 2 glaucoma specialists (S.A.K and H-Y.L.P). Each observer was blinded to the patient's clinical information and test results. Discrepancies between the two observers were resolved by consensus. We defined "DH in PPA" as an isolated hemorrhage that develops in the area of PPA. We divided the optic disc and its periphery into six sectors (the temporal, superotemporal, inferotemporal, nasal, superonasal, and inferonasal). The DHs on the optic disc or peripapillary area extending to the optic disc border at temporal regions were included in "DH in PPA/DH in temporal region" group. The DHs located on the optic disc and its margins at superotemporal and inferotemporal regions were classified as "typical DH". Alternative causes of hemorrhage were excluded by diagnostic testing for ischemic optic neuropathy, papillitis, retinal vein occlusion, diabetic retinopathy, and posterior vitreous detachment (PVD). As previous study, PVD-related DH showed higher frequency of flame shape, nasal location, and greater area compared to the glaucomatous DH<sup>15</sup>. We excluded DH in nasal location, and DH size and shape was carefully examined. Furthermore, eyes with PVD and subretinal hemorrhage was excluded examined by OCT.

### Swept-source optical coherence tomography

We used a swept-source (SS) OCT (DRI OCT Triton; Topcon). The central wavelength was 1050 nm, the acquisition speed was 100,000 A-scans/s, and the axial and transversal resolutions were 7 and 20  $\mu\text{m}$ , respectively. Only clear images with quality  $\geq 40$ , and which did not exhibit blurring because of motion and segmentation errors, were analyzed.

The  $\gamma$ -zone PPA was defined as the region between the end of Bruch membrane and the anterior scleral opening on SS OCT images. The OCT image of the macula served to determine the localization of the fovea, and the ONH imaging served for defining the border of  $\gamma$ -zone. The distance from the disc edge to the foveal center was measured from OCT images (Fig. 2).

The angle of scleral bending at the edge of scleral bending was measured on SS OCT images using ImageJ software (National Institutes of Health, Bethesda, Maryland). 2 tangent lines were drawn along the surface of the sclera on both sides of the scleral bending. The angle of scleral bending was measured as the angle between two tangential lines<sup>26</sup>. (Fig. 2) Two independent observers (S.A.K and H.Y.P), masked to the clinical data, independently identified the structural parameters. Disagreements were resolved by a third author (C.K.P).

### Measurement of optic disc ovality ratio, torsion degree, and peripapillary atrophy area

Optic disc ovality ratio in 2-dimensional photography was identified, which was calculated as the ratio between the longest and shortest diameters of the optic disc. Optic disc torsion was defined as the deviation degree of the long axis of the optic disc from the vertical meridian from fundus photography. The vertical meridian was identified as a vertical line 90° from the horizontal line connecting the fovea to the center of the optic disc. The torsion degree was indicated as a positive or negative value; a positive value noted the inferotemporal torsion direction, and a negative value noted the opposite direction. PPA area was defined as an inner crescent of chorioretinal atrophy with the visible sclera and choroidal vessels on fundus photograph images. PPA and clinical disc margin were plotted using a mouse-driven cursor to trace the disc and PPA margins directly onto the fundus photographs. Subsequently, the pixel areas of PPA were obtained using ImageJ. Two independent observers (S.A.K and H.Y.P), masked to the clinical data, independently identified all the structural parameters. Disagreements were resolved by a third author (C.K.P).

### Determination of glaucoma progression

Glaucoma progression measured by VF was determined using event- and trend-based analyses. In the event-based analyses, VF progression was considered if there was a significant deterioration of VF from the baseline pattern deviation at  $> 3$  of the same test points that were evaluated on 3 consecutive examinations. In the trend-based analyses, MD slope of VFs were calculated using linear regression analyses. Two examiners (S.A.K and H.-Y.L.P.) determined VF progression, and cases were excluded if the opinions of the 2 observers differed. To minimize the effect of subjectivity in VF testing, all patients were required to produce at least 5 reliable VF tests, and the first result was excluded from the calculation of the MD slope.

### Statistical analysis

Continuous variables were analyzed by Student *t* test. Categorical variables were compared using Chi-square test. To determine the factors associated with DH in PPA, univariate and multivariate logistic regression analyses were performed. Univariate and multivariate cox Proportional Hazard analyses were used to determine the

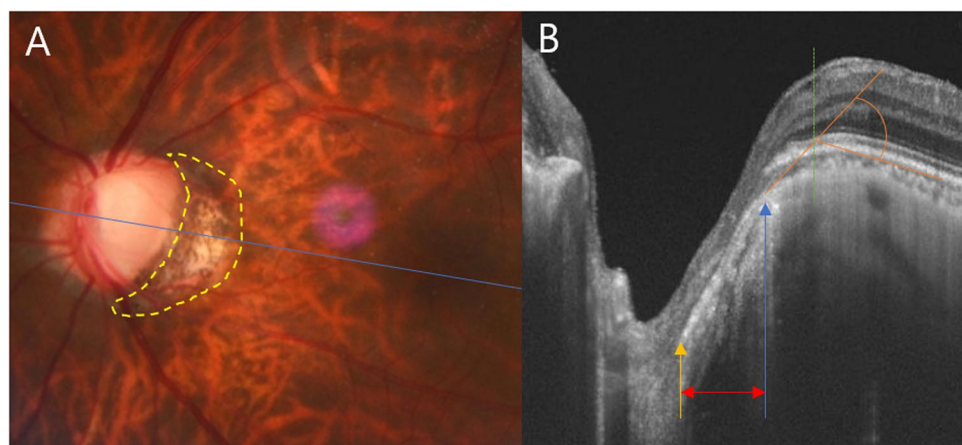


**Figure 2.** Measurements of the  $\beta$ - and  $\gamma$ -zone peripapillary atrophy (PPA) and angle of scleral bending. (A) The area of  $\beta$ -zone PPA was measured as an inner crescent of chorioretinal atrophy (dashed yellow line) on fundus photograph images. (B) The  $\gamma$ -zone PPA was measured as the distance between anterior scleral opening (yellow arrow) and Bruch membrane opening (blue arrow) on the optical coherence tomography image (along with the blue line in panel A). To measure the angle of scleral bending, 2 tangent lines were drawn along the surface of the sclera on both sides of the scleral bending (orange lines). The angle between the 2 lines was measured, as shown with an orange arch.

factors associated with VF progression among the eyes with and without DH in PPA, and the eyes with DH at different location. P value of  $< 0.10$  in the univariate model was included in the multivariate model. P values of  $< 0.05$  were considered statistically significant. All statistical analyses were performed with SPSS for Windows statistical software (version 16.0; SPSS Inc).

## Data availability

The datasets used and/or analysed during the current study available from the corresponding author on reasonable request.

Received: 14 May 2024; Accepted: 26 September 2024

Published online: 15 October 2024

## References

- Budenz, D. L. et al. Detection and prognostic significance of optic disc hemorrhages during the ocular hypertension treatment study. *Ophthalmology* **113**, 2137–2143. <https://doi.org/10.1016/j.ophtha.2006.06.022> (2006).
- Chung, E., Demetriades, A. M., Christos, P. J. & Radcliffe, N. M. Structural glaucomatous progression before and after occurrence of an optic disc haemorrhage. *Br J Ophthalmol* **99**, 21–25. <https://doi.org/10.1136/bjophthalmol-2014-305349> (2015).
- Ernest, P. J. et al. An evidence-based review of prognostic factors for glaucomatous visual field progression. *Ophthalmology* **120**, 512–519. <https://doi.org/10.1016/j.ophtha.2012.09.005> (2013).
- Bengtsson, B., Leske, M. C., Yang, Z. & Heijl, A. Disc hemorrhages and treatment in the early manifest glaucoma trial. *Ophthalmology* **115**, 2044–2048. <https://doi.org/10.1016/j.ophtha.2008.05.031> (2008).
- Drance, S., Anderson, D. R. & Schulzer, M. Risk factors for progression of visual field abnormalities in normal-tension glaucoma. *Am J Ophthalmol* **131**, 699–708. [https://doi.org/10.1016/s0002-9394\(01\)00964-3](https://doi.org/10.1016/s0002-9394(01)00964-3) (2001).
- Nitta, K. et al. Does the enlargement of retinal nerve fiber layer defects relate to disc hemorrhage or progressive visual field loss in normal-tension glaucoma?. *J Glaucoma* **20**, 189–195. <https://doi.org/10.1097/IJG.0b013e3181e0799c> (2011).
- Jonas, J. B., Martus, P., Budde, W. M. & Hayler, J. Morphologic predictive factors for development of optic disc hemorrhages in glaucoma. *Invest Ophthalmol Vis Sci* **43**, 2956–2961 (2002).
- Kim, Y. K., Jeoung, J. W. & Park, K. H. Effect of focal lamina cribrosa defect on disc hemorrhage area in glaucoma. *Investig Ophthalmol Vis Sci* **57**, 899–907 (2016).
- David, R. C. C. et al. Characteristics of central visual field progression in eyes with optic disc hemorrhage. *Am J Ophthalmol* **231**, 109–119. <https://doi.org/10.1016/j.ajo.2021.05.026> (2021).
- Park, H. L., Lee, J., Jung, Y. & Park, C. K. Optic disc hemorrhage and lamina cribrosa defects in glaucoma progression. *Sci Rep* **7**, 3489. <https://doi.org/10.1038/s41598-017-03828-0> (2017).
- Kim, Y. K., Park, K. H., Yoo, B. W. & Kim, H. C. Topographic characteristics of optic disc hemorrhage in primary open-angle glaucoma. *Invest Ophthalmol Vis Sci* **55**, 169–176. <https://doi.org/10.1167/iovs.13-13192> (2014).
- Kim, H. S., Park, K. H., Jeoung, J. W. & Park, J. Comparison of myopic and nonmyopic disc hemorrhage in primary open-angle glaucoma. *Jpn J Ophthalmol* **57**, 166–171. <https://doi.org/10.1007/s10384-012-0209-5> (2013).
- Ha, A., Kim, Y. K., Jeoung, J. W. & Park, K. H. Impact of optic disc hemorrhage on subsequent glaucoma progression in mild-to-moderate myopia. *PLoS One* **12**, e0189706. <https://doi.org/10.1371/journal.pone.0189706> (2017).
- Yamamoto, T., Iwase, A., Kawase, K., Sawada, A. & Ishida, K. Optic disc hemorrhages detected in a large-scale eye disease screening project. *J Glaucoma* **13**, 356–360. <https://doi.org/10.1097/01.jig.0000137436.68060.d2> (2004).
- Jin, C., Park, G. S., Kim, K. N., Song, M. Y. & Hwang, Y. H. Comparison of posterior vitreous detachment-related and glaucomatous optic disc hemorrhage. *Sci Rep* **13**, 5011. <https://doi.org/10.1038/s41598-023-32327-8> (2023).
- Xiong, J. et al. Papillary and peripapillary hemorrhages in eyes with pathologic myopia. *Invest Ophthalmol Vis Sci* **63**, 28. <https://doi.org/10.1167/iovs.63.12.28> (2022).
- Hsia, Y., Su, C. C., Wang, T. H. & Huang, J. Y. Clinical characteristics of glaucoma patients with disc hemorrhage in different locations. *Graefes Arch Clin Exp Ophthalmol* **257**, 1955–1962. <https://doi.org/10.1007/s00417-019-04379-y> (2019).
- Vurgese, S., Panda-Jonas, S. & Jonas, J. B. Scleral thickness in human eyes. *PLoS One* **7**, e29692. <https://doi.org/10.1371/journal.pone.0029692> (2012).
- Jonas, J. B., Ohno-Matsui, K., Panda-Jonas, S. & Myopia., Anatomic changes and consequences for its etiology. *Asia Pac J Ophthalmol (Phila)* **8**, 355–359. <https://doi.org/10.1097/01.APO.0000578944.25956.8b> (2019).
- Jonas, J. B., Fang, Y., Weber, P. & Ohno-Matsui, K. Parapapillary gamma and delta zones in high myopia. *Retina* **38**, 931–938. <https://doi.org/10.1097/iae.0000000000001650> (2018).
- Jonas, J. B., Jonas, S. B., Jonas, R. A., Holbach, L. & Panda-Jonas, S. Histology of the parapapillary region in high myopia. *Am J Ophthalmol* **152**, 1021–1029. <https://doi.org/10.1016/j.ajo.2011.05.006> (2011).
- Lee, E. J., Han, J. C. & Kee, C. A novel hypothesis for the pathogenesis of glaucomatous disc hemorrhage. *Prog Retin Eye Res* **60**, 20–43. <https://doi.org/10.1016/j.preteyeres.2017.08.002> (2017).
- Quigley, H. A., Addicks, E. M., Green, W. R. & Maumenee, A. E. Optic nerve damage in human glaucoma. II. The site of injury and susceptibility to damage. *Arch Ophthalmol* **99**, 635–649. <https://doi.org/10.1001/archophth.1981.03930010635009> (1981).
- Jonas, J. B. et al. Parapapillary gamma zone and axial elongation-associated optic disc rotation: the Beijing eye study. *Invest Ophthalmol Vis Sci* **57**, 396–402. <https://doi.org/10.1167/iovs.15-18263> (2016).
- Dai, Y., Jonas, J. B., Huang, H., Wang, M. & Sun, X. Microstructure of parapapillary atrophy: beta zone and gamma zone. *Invest Ophthalmol Vis Sci* **54**, 2013–2018. <https://doi.org/10.1167/iovs.12-11255> (2013).
- Akagi, T. et al. Peripapillary scleral deformation and retinal nerve fiber damage in high myopia assessed with swept-source optical coherence tomography. *Am J Ophthalmol* **155**, 927–936. <https://doi.org/10.1016/j.ajo.2012.12.014> (2013).
- Siegnier, S. W. & Netland, P. A. Optic disc hemorrhages and progression of glaucoma. *Ophthalmology* **103**, 1014–1024. [https://doi.org/10.1016/s0161-6420\(96\)30572-1](https://doi.org/10.1016/s0161-6420(96)30572-1) (1996).
- Leung, C. K. et al. Retinal nerve fiber layer imaging with spectral-domain optical coherence tomography: pattern of RNFL defects in glaucoma. *Ophthalmology* **117**, 2337–2344. <https://doi.org/10.1016/j.ophtha.2010.04.002> (2010).
- Yamagami, A. et al. Evaluation of the relationship between glaucomatous disc subtypes and occurrence of disc hemorrhage and glaucoma progression in open angle glaucoma. *Sci Rep* **10**, 21059. <https://doi.org/10.1038/s41598-020-77932-z> (2020).
- Ohno-Matsui, K. et al. Long-term development of significant visual field defects in highly myopic eyes. *Am J Ophthalmol* **152**, 256–265 (2011).
- Sonnsjö, B., Dokmo, Y. & Krakau, T. Disc haemorrhages, precursors of open angle glaucoma. *Prog Retin Eye Res* **21**, 35–56. [https://doi.org/10.1016/s1350-9462\(01\)00019-2](https://doi.org/10.1016/s1350-9462(01)00019-2) (2002).
- Lin, F. et al. Classification of visual field abnormalities in highly myopic eyes without pathologic change. *Ophthalmology* **129**, 803–812. <https://doi.org/10.1016/j.ophtha.2022.03.001> (2022).



### Author contributions

S.A.K. and H.-Y.L.P. conceptualized the research and wrote the main manuscript. S.A.K. and H.-Y.L.P. curated the dataset and analyzed the data. C.K.P. supervised the research. All authors reviewed the manuscript.

### Funding

No author has received financial support or has financial interest in any material or method mentioned.

### Declarations

### Competing interests

The authors declare no competing interests.

### Additional information

**Correspondence** and requests for materials should be addressed to H.-Y.L.P.

**Reprints and permissions information** is available at [www.nature.com/reprints](http://www.nature.com/reprints).

**Publisher's note** Springer Nature remains neutral with regard to jurisdictional claims in published maps and institutional affiliations.

**Open Access** This article is licensed under a Creative Commons Attribution-NonCommercial-NoDerivatives 4.0 International License, which permits any non-commercial use, sharing, distribution and reproduction in any medium or format, as long as you give appropriate credit to the original author(s) and the source, provide a link to the Creative Commons licence, and indicate if you modified the licensed material. You do not have permission under this licence to share adapted material derived from this article or parts of it. The images or other third party material in this article are included in the article's Creative Commons licence, unless indicated otherwise in a credit line to the material. If material is not included in the article's Creative Commons licence and your intended use is not permitted by statutory regulation or exceeds the permitted use, you will need to obtain permission directly from the copyright holder. To view a copy of this licence, visit <http://creativecommons.org/licenses/by-nc-nd/4.0/>.

© The Author(s) 2024